

## **Saturation by Noise and CW Signals in SIS Mixers**

A. R. Kerr

National Radio Astronomy Observatory<sup>1</sup>  
Charlottesville, VA 22903, USA

### **ABSTRACT**

In ALMA Memo 321, Plambeck points out that saturation (gain compression) is likely to be a significant factor limiting the calibration accuracy of ALMA observations. In this paper, saturation by broadband noise and CW signals is analyzed for representative SIS receivers operating at different frequencies. Many SIS mixers in current use are expected to exhibit a significant degree of gain compression when connected to a room-temperature source. Previous analyses of saturation in SIS mixers have applied only to CW signals. To analyze saturation by noise, the statistics of the output voltage are derived from those of the input signal. A single constant, applicable to all SIS mixers, is determined experimentally by fitting the predicted CW gain compression curve to measured data.

**Keywords:** Superconductor-Insulator-Superconductor mixers, saturation, gain compression, dynamic range.

### **1. INTRODUCTION**

Saturation (gain compression) can be a serious problem in SIS mixers not designed with appropriate input power levels in mind. Plambeck points out [1] that gain compression is likely to be a significant factor limiting the calibration accuracy of ALMA observations. SIS receivers have been reported with substantial gain compression at source temperatures as low as 50 K (1.4 dB compression [2]) and 300 K (1.7 dB compression [1]), while others have been capable of observing the sun (~6000 K) with only 0.6 dB gain compression [3]. Previous analyses of saturation in SIS mixers have considered only saturation by CW (sinusoidal) input signals. For amplifiers, it is well known that a given degree of saturation occurs at a lower input power level with noise than with a CW signal, and similar behavior is expected in SIS mixers. This memo describes a method for analyzing saturation by noise or CW signals in SIS mixers, and gives generalized saturation curves and representative results for mixers at several frequencies.

The established phenomenological theory of saturation by CW signals in SIS mixers is reviewed in Section 2, and shown to agree quite well with experimental data, even at gain compression levels as high as 3 dB.

When saturation is caused by broadband noise, a different approach is required, as described in Section 3, which allows the statistics of the output noise to be deduced from those of the input noise. The conclusion, not surprisingly, is that small and moderate degrees of gain compression are produced by noise powers several dB lower than the CW power required to produce the same gain compression. Many SIS mixers in current use are expected to exhibit a significant degree of gain compression when connected to a room-temperature source. It is noted that the linearity of a partly saturated SIS receiver to a small CW test signal can lead to the erroneous conclusion that the SIS mixer is not saturated by room-temperature input noise.

---

<sup>1</sup>The National Radio Astronomy Observatory is a facility of the National Science Foundation operated under cooperative agreement by Associated Universities, Inc.

## 2. ANALYSIS OF SATURATION BY A CW SIGNAL

For an SIS mixer with a well developed quantum response, the small signal power gain is a function of the bias voltage; this is evident in Fig. 1. Smith and Richards [4] argued that the large signal power gain could be considered as an average value of the small signal gain over an IF cycle.

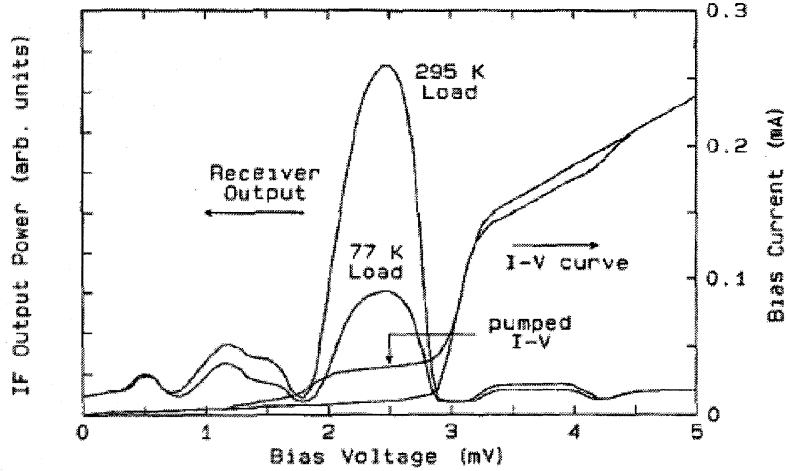


Fig. 1. I-V characteristics and output power vs. bias voltage curves for a 270 GHz SIS receiver. From [5].

The small signal power gain can be expanded as a Taylor series about the bias voltage  $V_0$  [6]:

$$G(v) = G(V_0) + (v - V_0)^2 G''(V_0) / 2. \quad (1)$$

If a CW input signal produces an output voltage  $v = V_0 + V_{IF} \sin(\omega_{IF} t)$ , the time-averaged gain is then

$$G = G_0 + V_{IF}^2 G''_0 / 4. \quad (2)$$

The IF power delivered to load  $R_L$  is  $P_{IF} = \frac{V_{IF}^2}{2R_L} = P_{in} G$ , from which it follows that [7]

$$G = G_0 \left( 1 + \frac{P_{sig}}{P_{sat}} \right)^{-1}, \quad (3)$$

where  $P_{sat} = -2 / G''_0 R_L$ . Because the degree of saturation of an SIS mixer depends only on the magnitude of the IF output voltage relative to the width of a photon step, *i.e.*,  $(G R_L P_{in})^{1/2}$  relative to  $Nhf/e$ , where  $N$  is the number of junctions in series and  $f$  is the LO frequency,  $P_{sat}$  can be written in the form

$$P_{sat} = K_{sat}^2 \left( \frac{hf}{e} \right)^2 \frac{N^2}{G_0 R_L} = C_{sat} \frac{N^2 f^2}{G_0 R_L}, \quad (4)$$

where  $K_{sat}^2$  and  $C_{sat}$  are constant for all SIS mixers.  $K_{sat}^2$  has been evaluated in [6] from experimental data which gives  $K_{sat}^2 = 0.10$ , corresponding to  $C_{sat} = 1.7e-30$ .

Figs. 2 and 3 show the results of saturation measurements on two SIS mixers using CW signals [7]. The saturation curve according to eq. (3) (the solid line) is seen to fit the measured data well. The value of  $P_{sat}$  is chosen to give the best fit to the data.

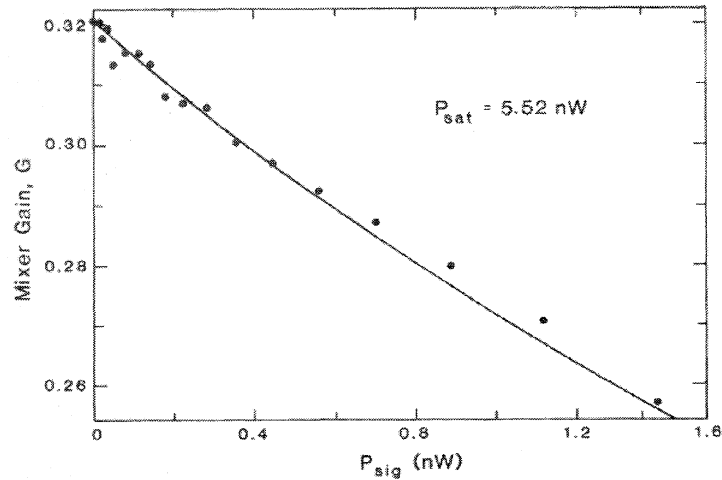


Fig. 2. Measured CW saturation for a 2-junction Pb/Ox/Nb SIS mixer at 115 GHz, from [7]. The solid curve is from eq. (3) with the value of  $P_{sat}$  chosen to give the best fit to the measured data.

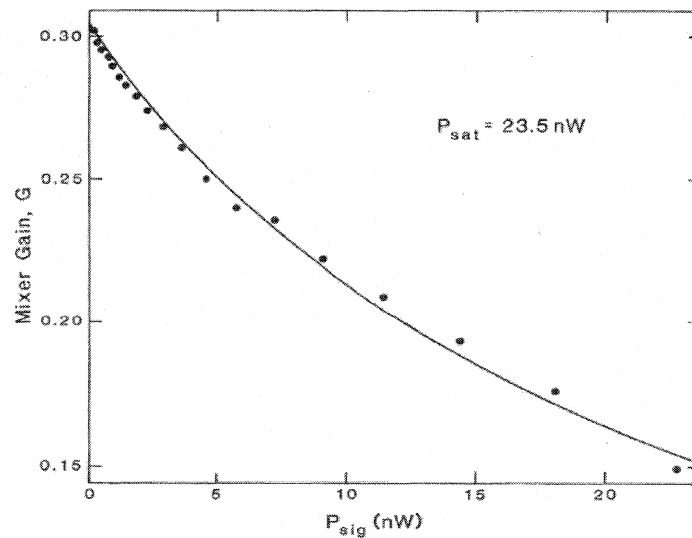


Fig. 3. Measured CW saturation for a 4-junction Nb/Al-AIOx/Nb SIS mixer at 115 GHz, from [7]. The solid curve is from eq. (3) with the value of  $P_{sat}$  chosen to give the best fit to the measured data.

Table I shows the values of  $C_{sat}$  obtained from measurements of the CW saturation power of four different SIS receivers. It is clear that the values of  $C_{sat}$  are reasonably close to the value  $1.7e-30$  above. Table II shows, for the same four SIS receivers, the CW signal power required to produce a gain compression of 1 dB and 1%.

**Table I —  $C_{sat}$  evaluated for four SIS mixers**

	LO GHz	Type	N	$R_n$	$L_{SSB}$ dB	$R_L$	$P_{sat}$ nW	$C_{sat}$
Pan <i>et al.</i> [8]	115	Pb-Nb	2	60	4.9	50	6.2	1.90E-30
Feldman <i>et al.</i> [7]	115	Pb-Nb	2	60	5.0	50	5.5	1.64E-30
Feldman <i>et al.</i> [7]	115	Nb	4	60	5.0	50	24	1.79E-30
Tong <i>et al.</i> [5]	270	Nb	1	18	3.0	50	6.4	2.20E-30

**Table II — CW saturation powers for the mixers in Table I**

	LO GHz	N	$L_{SSB}$ dB	$R_L$	$P_{1dB}$ nW	$P_{1\%}$ nW
Pan <i>et al.</i> [8]	115	2	4.9	50	1.6	0.062
Feldman <i>et al.</i> [7]	115	2	5	50	1.4	0.055
Feldman <i>et al.</i> [7]	115	4	5	50	6.2	0.240
Tong <i>et al.</i> [5]	270	1	3	50	1.7	0.064

### 3. ANALYSIS OF SATURATION BY BROADBAND NOISE

The previous section considered saturation caused by a sinusoidal RF input signal. When the RF input is noise, different saturation characteristics are expected. Because of the statistical nature of noise, the instantaneous amplitude of the signal at times exceeds the peak value of a CW signal having the same power, so gain compression begins at a lower power level than with a CW signal. To analyze gain compression by noise, it is convenient to consider the *voltage* gain of an SIS mixer rather than the *power* gain which was the focus in the previous section. If the probability density function of the input noise voltage is known, and also the nonlinear voltage characteristic of the gain compression mechanism, a new probability density function can be computed which characterizes the compressed output signal. In this section, this approach is applied to saturation by noise and CW signals — the latter case giving results in close agreement with those in the previous section.

The SIS mixer is characterized in Fig. 4 as a non-saturating mixer in series with a saturating IF element. The non-saturating mixer has gain and impedance characteristics, at all input power levels, identical to those of the actual mixer when operated under small signal conditions. The saturating element has an input impedance equal to the IF load impedance,  $R_L$ , an output impedance equal to that of the mixer,  $Z_m$ , and unity small-signal voltage gain when connected to the IF load. Hence, under small-signal and moderately large-signal operation, the circuit of Fig. 4 is indistinguishable from the real mixer.

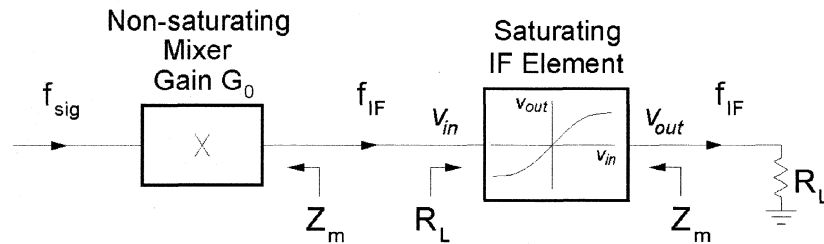


Fig. 4. Representation of the SIS mixer as a non-saturating mixer in series with a saturating IF element. The non-saturating mixer has gain and impedance characteristics identical to those of the actual mixer when operated under small signal conditions. The saturating IF element has unity small signal gain, an input impedance equal to the IF load impedance,  $R_L$ , and an output impedance equal to that of the mixer,  $Z_m$ .

The saturating element in Fig. 4 is characterized by its nonlinear voltage characteristic  $v_{out}(t) = f(v_{in}(t))$ , measured with the mixer and IF load in place. Note that  $v_{in}$  and  $v_{out}$  are the instantaneous values, not amplitudes, of the IF voltages at the input and output of the saturating IF element, as indicated in Fig. 4. When the mixer is biased near the middle of a photon step at the small-signal gain maximum,  $v_{out}$  is approximated by an odd function of  $v_{in}$ , and the differential gain of the saturating element is an even function of  $v_{in}$  which can be written, to first order, as<sup>2</sup>

$$A = \frac{dv_{out}}{dv_{in}} = \frac{1}{1 + A_3^2 v_{in}^2} \quad (5)$$

Since the degree of saturation of an SIS mixer depends only on the magnitude of the IF output voltage relative to the width  $Nhf/e$  of a photon step, it is convenient to use normalized input and output voltages:

$$V_{in} = \frac{e}{Nhf} v_{in} \quad \text{and} \quad V_{out} = \frac{e}{Nhf} v_{out} \quad (6)$$

<sup>2</sup> Other even functions could be chosen to approximate  $A(v_{in})$ , for example, the truncated Taylor expansion  $(1 + Bv^2)$ , which would give a good approximation to saturation in the real mixer for small values of  $v$ . It was found that the form of eq. (5),  $1/(1 + Bv^2)$ , gave good agreement with measured data even at levels of gain compression as high as 3 dB.

Then, in (5),

$$A(V_{in}) = \frac{dv_{out}}{dv_{in}} = \frac{dV_{out}}{dV_{in}} = \frac{1}{1 + C_3^2 V_{in}^2}, \quad (7)$$

where  $C_3$  is a constant, independent of  $N$  and  $f$ , for all SIS mixers. The instantaneous (large signal) normalized output voltage is then

$$V_{out}(t) = \int_0^{V_{in}} \frac{dV_{in}}{1 + C_3^2 V_{in}^2(t)} = \frac{1}{C_3} \arctan(C_3 V_{in}(t)), \quad (8)$$

and the instantaneous large-signal voltage gain is

$$A_{LS}(t) = \frac{v_{out}}{v_{in}} = \frac{V_{out}}{V_{in}} = \frac{\arctan(C_3 V_{in}(t))}{C_3 V_{in}(t)}. \quad (9)$$

When saturation is caused by broadband noise, eq. (9) allows the probability density function of the output noise to be computed from that of the input noise. The probability density of a Gaussian noise signal of mean square voltage  $\sigma^2$  is given by

$$p(v) = \frac{1}{\sigma\sqrt{2\pi}} \exp\left(-\frac{v^2}{2\sigma^2}\right). \quad (10)$$

For the circuit of Fig. 4, if  $\sigma_{in}$  is the RMS voltage at the input of the nonlinear element whose input impedance is  $R_L$ , then the power delivered to the nonlinear element  $P_{in} = G_0 P_{sig} = \sigma_{in}^2/R_L$ . The output power delivered to the IF load  $R_L$  is

$$P_{out} = GP_{sig} = \frac{1}{R_L} \int_{-\infty}^{\infty} v_{out}^2 p(v_{in}) dv_{in}, \quad (11)$$

where  $v_{out}(v_{in})$  is given by eq. (9). Therefore,

$$\frac{G}{G_0} = \frac{1}{\sigma^2} \int_{-\infty}^{\infty} v_{out}^2 p(v_{in}) dv_{in}. \quad (12)$$

Normalizing voltages to  $Nhf/e$  as in eq. (6), and defining the normalized RMS voltage at the input of the saturating element as  $S_{in} = \frac{e}{Nhf} \sigma_{in}$ , eqs. (8), (10) and (12) give

$$\frac{G}{G_0} = \frac{1}{\sqrt{2\pi} C_3^2 S_{in}^3} \int_{-\infty}^{\infty} \arctan^2(C_3 V_{in}) \exp\left(-\frac{V_{in}^2}{2S_{in}^2}\right) dV_{in}. \quad (13)$$

Since  $S_{in}^2 = \left(\frac{e}{Nhf}\right)^2 \sigma_{in}^2 = \left(\frac{e}{Nhf}\right)^2 G_0 P_{sig} R_L$ , eq. (13) allows  $G/G_0$  to be computed as a function of  $P_{sig}$ ,

$G_0$ ,  $R_L$ ,  $f$ , and  $N$ . If the input noise is from a broadband source with noise temperature  $T_{sig}$  at the input of the receiver, then  $P_{sig} = 2kT_{sig}B_1$ , the factor 2 accounting for the noise received in both upper and lower sidebands of the receiver. Determination of the constant  $C_3$  is described in the next section, and the appropriate value of the effective IF bandwidth  $B_1$  is discussed in Section 4.

### Determination of $C_3$

To determine the constant  $C_3$ , saturation by a CW signal was analyzed using (9), and  $C_3$  adjusted to fit the experimental results given in the previous section.

A CW RF input signal of power  $P_{sig}$  delivers power  $P_{in} = G_0 P_{sig}$  to the input resistance  $R_L$  of the saturating element in Fig. 4. If the voltage at the input of the saturating IF element is  $v_{in}(t) = a \sin(\omega_{IF} t)$ , then

$$P_{in} = G_0 P_{sig} = a^2 / 2 R_L. \quad (14)$$

The instantaneous output power delivered to the IF load is  $P_{out}(t) = v_{out}^2(t) / R_L$ , which has an average value over the IF period

$$P_{out} = G P_{sig} = \frac{1}{R_L} \frac{1}{\tau_{IF}} \int_0^{\tau_{IF}} v_{out}^2(t) dt. \quad (15)$$

From eqs. (14) and (15):

$$\frac{G}{G_0} = \frac{2}{a^2} \frac{1}{\tau_{IF}} \int_0^{\tau_{IF}} v_{out}^2(t) dt. \quad (16)$$

Using normalized voltages, as in eq. (6), eq. (8) gives

$$\frac{G}{G_0} = \frac{2}{A^2 C_3^2} \frac{1}{\tau_{IF}} \int_0^{\tau_{IF}} \arctan^2(C_3 A \sin(\omega_{IF} t)) dt, \quad (17)$$

where  $A = \frac{e}{N h f} a$  is the normalized amplitude of  $v_{in}$ . Eq. (17) describes saturation by a CW signal

in any SIS mixer. Since  $A^2 = 2 \left( \frac{e}{N h f} \right)^2 R_L G_0 P_{sig}$ , eq. (17) allows  $G/G_0$  to be computed as a function of  $P_{sig}$ ,  $G_0$ ,  $R_L$ ,  $f$ , and  $N$ .

To determine the constant  $C_3$ , saturation by a CW signal was analyzed using (17), and  $C_3$  adjusted to fit the experimental results given in the previous section. A good fit to the measured data at low saturation levels is obtained with  $C_3 = 3.3$ . Fig. 5 shows the agreement between eq. (3) with  $P_{sat} = 23.5$  nW, which closely fits the measured saturation data for the 115 GHz 4-junction mixer, and the saturation characteristic given by eq. (9) with  $C_3 = 3.3$ .

In the above approach, the degree of gain compression was determined from the mean power delivered to the IF load (eqs.(15)-(17)). It could also be determined using the fundamental Fourier component of the power delivered to the IF load. We found that these two methods of calculation had negligible difference for gain compression levels up to ~50%.

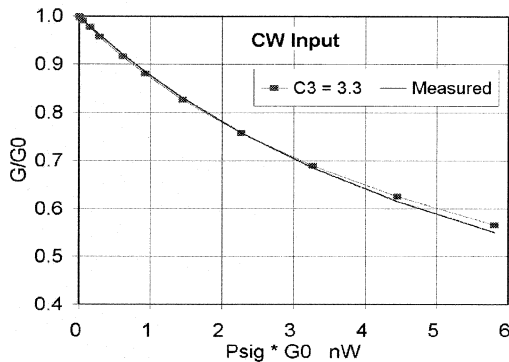


Fig. 5. The graph shows the close agreement between eq. (17) with  $C_3 = 3.3$  and Eq. (3) with  $P_{sat} = 23.5$  nW. Eq. (3) was shown to be an excellent fit to the measured gain compression curve for a 115 GHz 4-junction SIS mixer [7] (see Fig. 3).

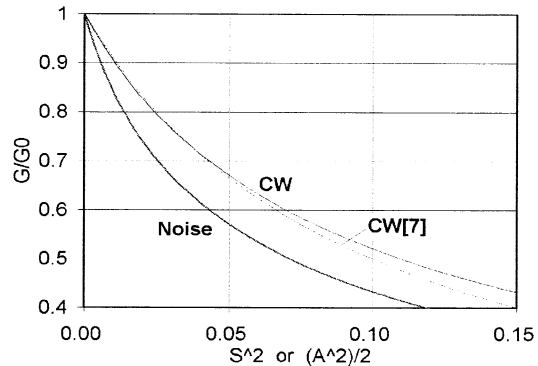


Fig. 6. Saturation by noise and CW signals. For noise,  $S^2$  is given by eq. (18), and for CW,  $A^2/2$  is given by eq. (19). The curve labeled CW[7] is computed from eq. (3) as in [7].

#### Comparison of Saturation by Noise and CW

A comparison of saturation by broadband noise and CW signals of equal powers is possible using eqs. (13) and (17). For noise, the signal power (in both sidebands)  $P_{sig}$  is related to  $S_{in}$  by

$$S_{in}^2 = \left( \frac{e}{Nh\nu} \right)^2 G_0 P_{sig} R_L, \quad (18)$$

and for a CW signal  $P_{sig}$  is related to  $A$  by

$$\frac{A^2}{2} = \left( \frac{e}{Nh\nu} \right)^2 G_0 P_{sig} R_L, \quad (19)$$

where  $N$  is the number of SIS junctions in series,  $G_0$  is the small-signal gain of the mixer, and  $R_L$  is the IF load resistance. Fig. 6 shows  $G/G_0$  as a function of  $S_{in}^2$  (for noise) and  $A^2/2$  (for CW). Also shown for comparison is the saturation curve computed from eq. (3) as in [7], which has been shown to fit experimental data well in the range  $0.5 \leq G/G_0 \leq 1$  (see Figs. 2 and 3).

#### Examples

To illustrate the degree to which gain compression is likely to affect SIS receiver calibration when using a room-temperature calibration load, we make the following assumptions: (i) The mixer input bandwidth is  $B_I$  in each sideband, with  $B_I$  equal to 20% of the LO frequency. Roughly, this corresponds to a receiver which downconverts all frequencies within the full RF waveguide band, half in the LSB and half in the USB, to an extended IF band from 0 to  $B_I$  Hz. (ii) The IF load on the mixer is taken as  $R_L = 50$  ohms over the extended IF band  $0 < f < B_I$ , an approximation which will be discussed below. An IF impedance of 50 ohms is used because this is the nominal input impedance of many low noise IF preamplifiers, including the present NRAO 4-12 GHz HFET preamplifier [9]. We assume the mixer and preamplifier are connected directly together with no intervening impedance transformer. (iii) The small-signal gain has a constant value  $G_0$  over the full input band  $0.8f_{LO} < f < 1.2f_{LO}$ . Under these assumptions, Fig. 7 shows the expected gain compression caused by a room-temperature calibration load for SIS mixers at four LO frequencies. The gain compression



produced by a CW input signal of the same power as the noise input is shown for comparison. It is seen from Fig. 7 that mixer receivers satisfying assumptions (i)-(iii), with small signal gain  $G_0 = 6$  dB SSB and a single SIS junction, can be expected to have a gain compression due to a room-temperature source of 16% at 115 GHz and 5% at 460 GHz. With four junctions, the gain compression is 1.4% at 115 GHz and 0.4% at 460 GHz.

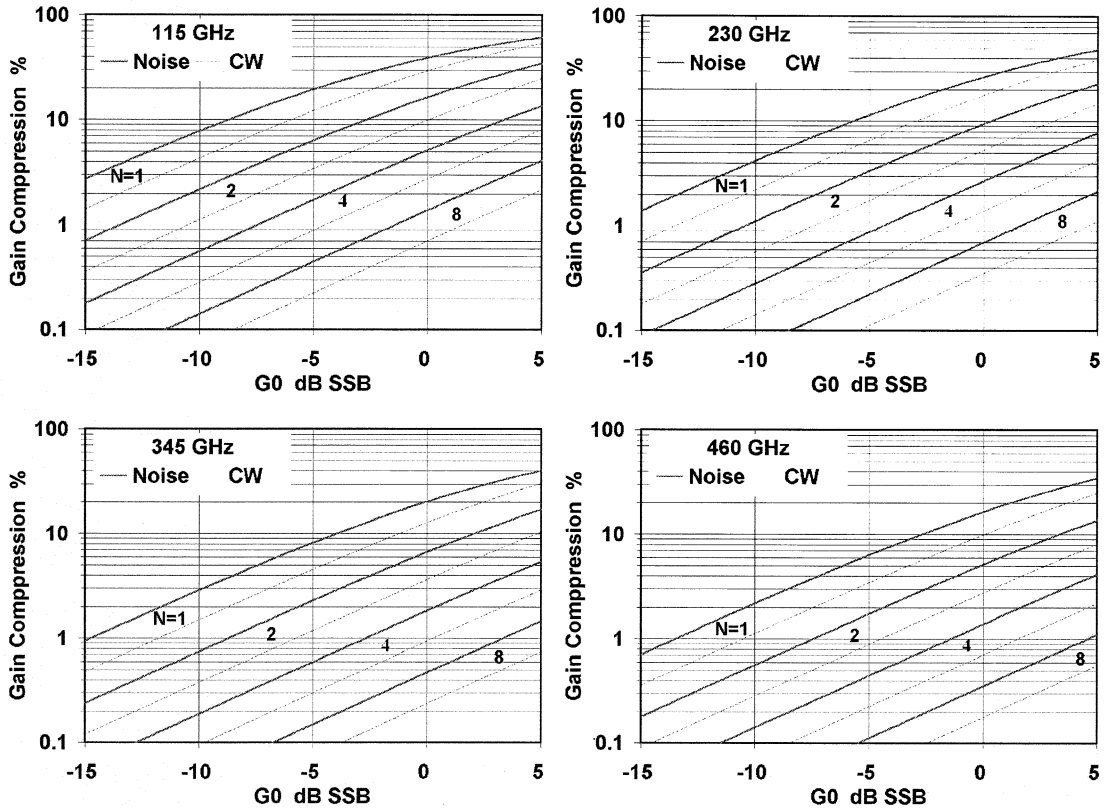


Fig. 7. Curves of gain compression caused by a 300 K source (solid red lines), as a function of small-signal mixer gain,  $G_0$ , for SIS mixers at four frequencies. The parameter  $N$  is the number of junctions in series. In all cases: (i) the input noise bandwidth  $B_i$  in each sideband is equal to 20% of the LO frequency, (ii) the IF load impedance is 50 ohms over the extended IF band  $0 < f_{IF} < B_i$ , and (iii) the small-signal gain is constant over  $0.8 f_{LO} < f_{sig} < 1.2 f_{LO}$ . Shown for comparison is the gain compression by a CW signal of the same power (dotted black line).

#### 4. DISCUSSION

It is clear from the simulations in Section 3 that noise and CW signals of equal power produce different degrees of saturation in SIS mixers. Furthermore, it is apparent that a room-temperature source may cause significant gain compression in many practical SIS receivers, a phenomenon which affects the accuracy of astronomical observations made with an SIS receiver calibrated using a room-temperature source.

### Bandwidth and IF Load Impedance

The noise saturation results in Fig. 7 are based on the following major assumptions: (i) the input noise bandwidth  $B_I$  in each sideband is equal to 20% of the LO frequency, (ii) the IF load impedance  $R_L = 50$  ohms over the frequency range 0 to  $B_I$ , and (iii) the small-signal gain  $G_o$  is flat over  $0.8 f_{LO} < f_{sig} < 1.2 f_{LO}$ . The frequency range  $0.8 f_{LO} < f_{sig} < 1.2 f_{LO}$  corresponds approximately to a standard waveguide band when  $f_{LO}$  is at the band center. A typical broadband waveguide to TEM mode transducer has poor coupling outside the waveguide band, and thus acts to some extent as a band-limiting filter. However, as saturation in SIS mixers is primarily determined by the magnitude of the output voltage, the behavior of the embedding impedance  $Z_e(f_{IF})$  over  $0 < f_{IF} < B_I$  seen by the SIS junction(s) is the major determinant of the saturation behavior. In the analysis, it has been assumed that  $Z_e = R_L$  at all frequencies, whereas in reality  $Z_e$  depends on the RF choke circuit of the mixer, any circuit elements between the mixer and IF amplifier, and the input impedance of the IF amplifier itself. The importance of  $Z_e$  over this extended IF range has been pointed out in [10].

### Improving the Dynamic Range

Are there ways to improve the dynamic range of an SIS receiver? It is clear, from eqs. (3) and (4) in the case of CW signals, and eqs. (6) and (9) in the case of noise, that the dynamic range of an SIS mixer can be increased by: (i) increasing the number  $N$  of junctions in series, (ii) reducing the transducer gain  $G_o$ , or (iii) reducing the IF load resistance  $R_L$  (which also affects  $G_o$ ). If saturation is caused by broadband noise, a bandpass or lowpass IF filter immediately following the SIS mixer could reduce the RMS IF noise voltage at the mixer output if the filter were designed to have low impedance at all frequencies above the desired IF band. This has been suggested in [10] but is difficult to implement unless the filter is incorporated into the SIS mixer chip. In [11], a 200-280 GHz SIS mixer is described in which  $|Z_e| < 50$  ohms over 0 to 150 GHz when the IF amplifier has an impedance of 50 ohms over that band (in reality, of course, the impedance of the IF amplifier is unlikely be 50 ohms at frequencies far from the nominal IF band). Fig. 8 shows  $Z_e(f)$  for that mixer, including the effects of the RF choke, junction capacitance, and all the RF circuit elements. The decrease of  $|Z_e|$  with frequency reduces the IF voltage at the mixer output due to a broadband noise input, and thereby reduces the degree of saturation compared with a mixer in which the IF embedding impedance is largely in the high impedance region of the chart.

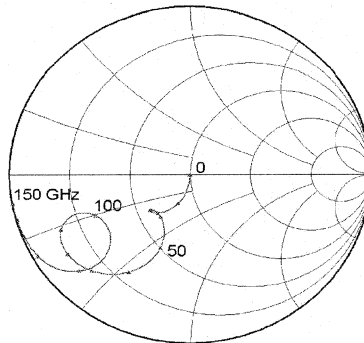


Fig. 8. Embedding impedance  $Z_e(f)$  seen by the SIS junctions in a low-parasitic 200-280 GHz SIS mixer [11].  $Z_e(f)$  includes the RF choke and all the RF circuit elements, and assumes that the input impedance of the IF amplifier is 50 ohms at all frequencies.  $Z_e$  is plotted on a 50-ohm Smith chart over the frequency range 0-150 GHz with markers every 10 GHz.

In principle, the dynamic range of an SIS mixer can be increased by increasing the junction area by a factor  $M (> 1)$  while reducing the embedding impedance at all frequencies by the same factor  $M$ ; for example, the larger junction could be connected to the same embedding circuit through an ideal transformer with impedance ratio  $M$  at all frequencies. A given degree of gain compression occurs in both the original mixer and the modified mixer when each has the same IF voltage at the junction. However, the modified mixer has an IF load impedance (seen from the junction) lower by factor  $M$  than the original mixer, so the IF power delivered to the load is larger by factor  $M$ , and the RF input power is therefore also larger by a factor  $M$ .

#### Measurement of Gain Compression using a CW Signal in the Presence of Broadband Noise

It is of interest to consider the response of an SIS mixer, partly saturated by broadband noise, to a small CW test signal. The test signal produces a response with a small-signal gain which is a function of the total input power (test signal + noise). The gain is not substantially affected by the test signal as long as its power is small compared with the noise input power, and the small-signal response is then linear. Only when the test signal power approaches that of the broadband input noise power in RF bandwidth  $2B_i$  ( $B_i$  is the effective IF noise bandwidth as defined above, and the factor 2 accounts for the two RF sidebands in a DSB mixer) will it contribute substantially to saturation, which will be evident from the nonlinearity of the curve of test signal output power vs test signal input power.

It is sometimes assumed that a linear curve of test signal output power vs test signal input power implies that a receiver is not saturated by broadband noise accompanying the test signal. This is the assumption in [5], for a receiver with a room temperature input load in which no gain compression was measured at low CW powers. It was concluded that "*...the receiver is still highly linear when subjected to radiation from an ambient load...*" If one applies the noise saturation analysis of Section 3 to the mixer used in [5], assuming an extended IF noise bandwidth  $B_i$  of 15 GHz, a room temperature black body source is predicted to produce ~5% gain compression — this is consistent with the other data given in [5].

To determine the degree of gain compression produced by broadband input noise, a small CW test signal can be used as an indicator. The small-signal gain curve (test signal output power vs test signal input power) is measured first, in the presence of the high level broadband noise source (*e.g.*, a room temperature load), and a convenient signal level in the linear region of this curve is chosen. Then, the high level noise source is replaced with a low level noise source (*e.g.*, a liquid nitrogen load) and the test signal output level re-measured. Any gain compression caused by the high level noise source will be indicated by an increase in the test signal output when the high level noise source is replaced with the low level noise source.

#### Balanced and Sideband Separating Mixers

In balanced mixers and sideband-separating mixers, the input power is divided equally between two unit (double-sideband) mixers. The power required to produce a given degree of gain compression is therefore twice that required to produce the same gain compression in a single unit mixer connected to the same signal and IF embedding impedances. In the case of a balanced sideband-separating mixer, the input power is divided between four unit mixers, so the saturation power is four times that of the unit mixer.

## ACKNOWLEDGMENTS

The author thanks Shing-Kuo Pan of NRAO and Charles Cunningham of HIA for their valuable discussions on saturation in SIS mixers and comments on the manuscript.

## REFERENCES

- [1] R. L. Plambeck, "Receiver amplitude calibration for ALMA," ALMA Memo 321, August 27, 2000. Available at <http://www.alma.nrao.edu/memos/>.
- [2] L. R. D'Addario, "An SIS Mixer for 90-120 GHz with Gain and Wide Bandwidth," *Int. J. Infrared Millimeter Waves*, vol. 5, no. 11, pp. 1419-1442, 1984.
- [3] E. S. Palmer, T. Dame, private communication, November 2001. The mixer used two SIS junctions in series and was tuned for SSB operation using its two waveguide tuners.
- [4] A. D. Smith and P. L. Richards, "Analytic solutions to SIS quantum mixer theory," *J. Appl. Phys.*, vol. 53, no. 5, pp. 3806-3812, May 1982.
- [5] C.-Y. E. Tong, R. Blundell, S. Paine, D. C. Papa, J. Kawamura, J. Stern, and H. G. LeDuc, "Design and Characterization of a 250-350 GHz Fixed-Tuned Superconductor-Insulator-Insulator Receiver," *IEEE Trans. Microwave Theory Tech.*, vol. MTT-44, no. 9, pp. 1548-1556, Sept. 1996.
- [6] M. J. Feldman and L. R. D'Addario, "Saturation of the SIS direct detector and the SIS mixer," *IEEE Trans. Magnetics*, vol. MAG-23, no. 2, pp. 1254-1258, March 1987.
- [7] M. J. Feldman, S.-K. Pan, and A.R. Kerr, "Saturation of the SIS mixer," *International Superconductivity Electronics Conference Digest*, Tokyo, pp. 290-292, Aug. 1987.
- [8] S.-K. Pan, A. R. Kerr, M. J. Feldman, A. Kleinsasser, J. Stasiak, R. L. Sandstrom, and W. J. Gallagher, "An 85-116 GHz SIS receiver using inductively shunted edge-junctions," *IEEE Trans. Microwave Theory Tech.*, vol. MTT-37, no. 3, pp. 580-592, March 1989.
- [9] E. F. Lauria, A. R. Kerr, M. W. Pospieszalski, S.-K. Pan, J. E. Effland, and A. W. Lichtenberger, "A 200-300 GHz SIS Mixer-Preamplifier with 8 GHz IF Bandwidth," *2001 IEEE International Microwave Symposium Digest*, pp. 1645-1648, May 2001. Available as ALMA Memo 378 at <http://www.alma.nrao.edu/memos/>.
- [10] L. R. D'Addario, "Saturation of the SIS mixer by out-of-band signals," *IEEE Trans. Microwave Theory Tech.*, vol. MTT-26, pp. 1103-1105, no. 6, June 1988.
- [11] A. R. Kerr, S.-K. Pan, A. W. Lichtenberger and H. H. Huang, "A Tunerless SIS mixer for 200-280 GHz with low output capacitance and inductance," *Proceedings of the Ninth International Symposium on Space Terahertz Technology*, pp. 195-203, 17-19 March 1998. Available as ALMA Memo 205 at <http://www.mma.nrao.edu/memos/>.